ACS Catalysis

Research Article

pubs.acs.org/acscatalysis

# Multi-Layer Functionalized Poly(Ionic Liquid) Coated Magnetic Nanoparticles: Highly Recoverable and Magnetically Separable Brønsted Acid Catalyst

Ali Pourjavadi,* Seyed Hassan Hosseini, Maliheh Doulabi, Seyed Mahmoud Fakoorpoor, and Farzad Seidi

Polymer Research Laboratory, Department of Chemistry, Sharif University of Technology, Tehran, Iran

Supporting Information

**ABSTRACT:** A functionalized poly(ionic liquid) coated magnetic nanoparticle ($Fe_3O_4$@PIL) catalyst was successfully synthesized by polymerization of functionalized vinylimidazolium in the presence of surface modified magnetic nanoparticles. The resulting heterogeneous catalyst is shown to be an efficient acidic catalyst for synthesis of 1,1-diacetyl from aldehydes under solvent free conditions and room temperature in high yields. Also, the catalyst shows good activity for the deprotection reaction of acylals. After completion of reaction, the catalyst was simply recovered by an external conventional magnet and recycled without significant loss in the catalytic activity. Because of the polymer layers coated surface of the magnetic nanoparticles, the catalyst has a good thermal stability and recyclability. The poly(ionic liquid) coated magnetic nanoparticles represents a novel class of heterogeneous catalyst which are particularly attractive in the practice of organic synthesis in an environmentally friendly manner.

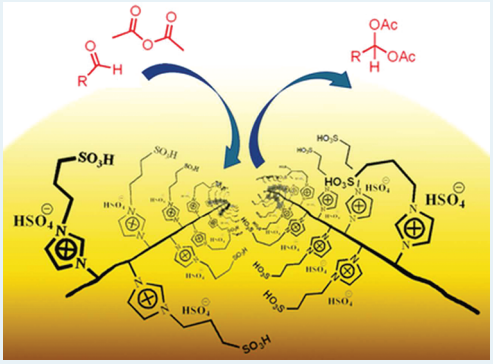

**KEYWORDS:** *magnetic catalysts, polymer coated magnetic nanoparticles, poly(ionic liquid), brønsted acid catalyst, diacetylation*

## INTRODUCTION

A restriction on the use of homogeneous catalysts in industry is the difficulty in separating the catalyst from the reaction mixture or separating the product continuously. It will be important economically and environmentally which catalyst in large-scale organic synthesis could be simply recycled. Use of heterogeneous catalysts would be an attractive solution to this problem because of their easy separation and facile recycling.[1,2] However, homogeneous catalysts show higher activity than heterogeneous catalysts, but heterogeneous catalyst seems to be more suitable for industrial process. To successfully obtain a highly active heterogeneous catalyst, a rational choice is immobilization of homogeneous catalyst on a variety of insoluble support materials. Many support materials are often used for immobilization of active homogeneous catalysts such as polymers,[3,4] zeolite,[5−9] silica,[10,11] or metal oxides.[12−15] Among these support materials, magnetic nanoparticles are very popular when used for immobilization of active homogeneous catalyst because their magnetic response causes simple separation of catalyst by using an external magnet. However magnetic nanoparticles always tend to undergo agglomeration because of the magnetic dipole−dipole attractions between particles; it was reported that formation of a passive coating of inert materials such as polymers on the surfaces of iron oxide nanoparticles could help to prevent their aggregation in solvents and improve their chemical stability.[16] Many kinds of catalysts were immobilized on the magnetic nanoparticles, such as enzymes,[17−19] polymers,[20−22] ionic liquids,[23−26] and acid catalysts.[27−29] However these catalysts have some disadvantages, such as low catalyst activity, low loading, high cost for large scale preparation, and need for toxic, flammable, environmentally hazardous organic solvents for purification of catalyst or reaction solvent. Therefore, finding a suitable method for the preparation of green catalysts is still an active research field.

On the other hand, ionic liquids (IL) have been described as one of the most promising new green materials.[30] Though ILs have some advantages, their widespread utilization is still limited by several drawbacks such high viscosity and homogeneity which makes it difficult to separate them and high cost for the use of relatively large amounts of ILs.[31,32] To solve this disadvantage, supported IL materials become more interesting and have found desirable application as solid organocatalysts. This class of advanced materials possesses the properties of ILs and behaves as bulk ILs.

The major problem with using heterogeneous catalysts is low loading of homogeneous catalyst onto the large amount of solid bed. In the normal grafting of organic compound onto the solid substrate only one layer of organic compound can be coated onto the surface. Therefore loading cannot be too high, and a large amount of solid catalyst should be used for the catalyzing process. Use of a large amount of heterogeneous catalysts has

Received: February 27, 2012
Revised: May 8, 2012
Published: May 10, 2012

   dx.doi.org/10.1021/cs300140j | ACS Catal. 2012, 2, 1259−1266

some disadvantages. Increasing the amount of catalyst causes more pollution of the reaction medium, and a larger amount of solvent will be required for reaction, separation process, and recovery of catalyst. Also in the conventional grafting of materials onto the solid surface, degradation of supported material by using several times, decreases reusability of catalyst. Thus, the development of a simple method for the preparation of catalyst with high loading levels has been needed. However mesoporous silicas with high surface area proportionally resolved this problem, but they have some disadvantage too. A serious problem concerning mesoporous silicas is their low hydrothermal stability, because of the hydrolysis of Si−O−Si bonds that were caused by the water adsorbed on the silanol groups.[33] As far as we know, a few papers were published about polymeric acid catalysts.[34−37]

Herein, we report the synthesis of a new class of acid heterogeneous magnetic catalyst in which magnetic nanoparticles were coated by multilayers of poly sulfonic acid functionalized imidazolium IL and used in the chemoselective synthesis of 1,1-diacetyls efficiently. At the end of reaction the catalyst can be easily separated by an external magnet, without using extra organic solvents and additional filtration steps. Selective protection and deprotection of carbonyl groups are valuable and simple protocols for manipulation of other functional groups during multistep syntheses. Protection/deprotection of aldehydes as acylals is often preferred because of their ease of preparation and their stability toward basic and neutral conditions.[38] Generally, they are synthesized from acetic anhydride and aldehydes using strong protonic acids,[39] Lewis acids,[40] and supported reagents.[41]

## RESULTS AND DISCUSSION

**Synthesis of Modified Magnetic Nanoparticles.** The magnetic ($Fe_3O_4$) nanoparticle was synthesized by the coprecipitation technique based on a reported method.[42] $FeCl_2{\cdot}4H_2O$ and $FeCl_3{\cdot}6H_2O$ were dissolved in ultrapure water under $N_2$ atmosphere and vigorous stirring (600 rpm). Then a $NH_3$ solution was added dropwise to the stirring mixture at room temperature, immediately followed by the addition of $NH_3$ solution, and a black precipitate was formed and the pH of solution adjusted between 11 and 12. The resulting black solution was vigorously stirred for 1 h at room temperature and $N_2$ atmosphere. The magnetic nanoparticles were then purified by a magnet, decantation and redispersion cycle 3 times, until a stable black magnetic dispersion was obtained.

Before coating of polymer onto the $Fe_3O_4$ surface, the surface of magnetic nanoparticles should be modified with 3-methacryloxypropyltrimethoxy-silane (MPS) to give active vinyl groups on the surface of $Fe_3O_4$. The presence of methacrylate groups on the surface of $Fe_3O_4$ makes polymerization easier on the surface of magnetic nanoparticles. On the other hand that causes copolymers grafted by covalent bonding to surface of $Fe_3O_4$. Coating of the surface of magnetic nanoparticles with methacrylate groups causes all magnetic nanoparticles grafted with copolymer shell. Without MPS-modification, only a minor part of the magnetic nanoparticles can be coated with a complete layer of polymer chains.[43]

**Synthesis of Catalyst ($Fe_3O_4$@PIL).** The procedure for synthesis of monomer 1-vinyl-3-(3-sulfopropyl) imidazolium hydrogen sulfate ([VSim][$HSO_4$]) and cross-linker 1,4-butanediyl-3,3′-bis-l-vinylimidazolium hydrogen sulfate ([BVD]) is shown in Scheme 1. [VSim][$HSO_4$] was

**Scheme 1. Synthesis Route to the Monomer and Cross-Linker Agent**

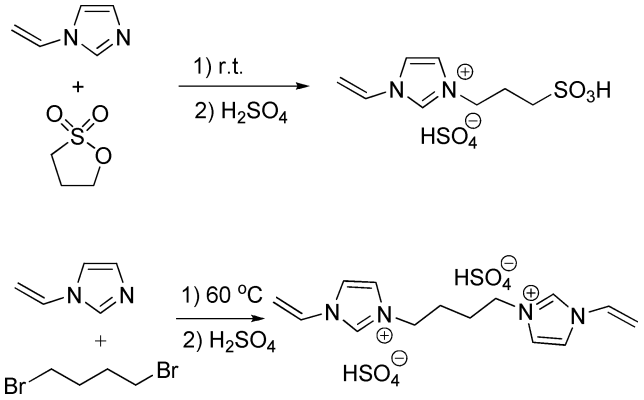


synthesized by the quaternization of l-vinylimidazole with 1,3-propanesultone according to the procedures given in the Experimental Section. After quaternization of vinylimidazole, sulfuric acid was used for neutralization of the inner salt. For preparation of [BVD], quaternization was performed by 1,4-dibromobutane and 2 equiv of vinylimidazole. Afterward, bromides ion was exchanged with hydrogen sulfate ions by sulfuric acid. It was found that both ([VSim][$HSO_4$]) and ([BVD]) were obtained pure in high yield as confirmed by FT-IR and $^1$H NMR (Supporting Information).

The procedure for synthesis of magnetic nanoparticle coated multilayered poly(1-vinyl-3-(3-sulfopropyl)-imidazolium hydrogen sulfate), noted as $Fe_3O_4$@PIL is depicted in Scheme 2. The advantage of a multilayered (or high loaded) poly(IL) catalysts could arise from the possibility that such catalysts could have a large amount of sulfuric acid functionalized IL species onto the surface. Such an approach could furnish catalysts to be used in a low weight% compared to the substrates. This is certainly useful for large-scale applications. Coating of poly IL layers (PIL) onto the $Fe_3O_4$@MPS was performed by distillation-precipitation polymerization with $Fe_3O_4$@MPS as the solid bead. Polymerization was initiated by AIBN in methanol at 70 °C. As copolymers are insoluble in the methanol (because of cross-linking) the generated copolymers will continuously precipitate from the solution and attach to the surface of the magnetic nanoparticles to form a multilayered shell. The loading of the copolymer shell can be precisely tailored by adjusting the concentration of the monomer and cross-linking agent while keeping the amount of $Fe_3O_4$@MPS nanoparticles and solvent constant. Three samples were synthesized, and recipes are listed in Table 1. As expected, the layer thickness or organic components will increase in the $Fe_3O_4$ surface with increasing monomer and cross-linker concentrations. Increasing the monomer or cross-linker concentration causes the precipitation process to occur faster in solution and more copolymer chains to attach to the surface of magnetic nanoparticles. We used $Fe_3O_4$@PIL (III) as catalyst because of the high loading level of polymer chains.

At the end of polymerization, catalyst was magnetically separated and washed several times with water and methanol to ensure unreacted monomer, cross-linker, and ungrafted copolymers dose not remain on the surface of magnetic nanoparticles. After separation of the catalyst, to remove any uncoated magnetic nanoparticles, the catalyst was treated with sulfuric acid. Uncoated magnetic nanoparticles were dissolved, and catalyst was washed again several times with water and


dx.doi.org/10.1021/cs300140j | ACS Catal. 2012, 2, 1259−1266

**Scheme 2. Synthesis of Multi-Layer Poly(IL) Coated Magnetic Nanoparticles ($Fe_3O_4$@PIL)**

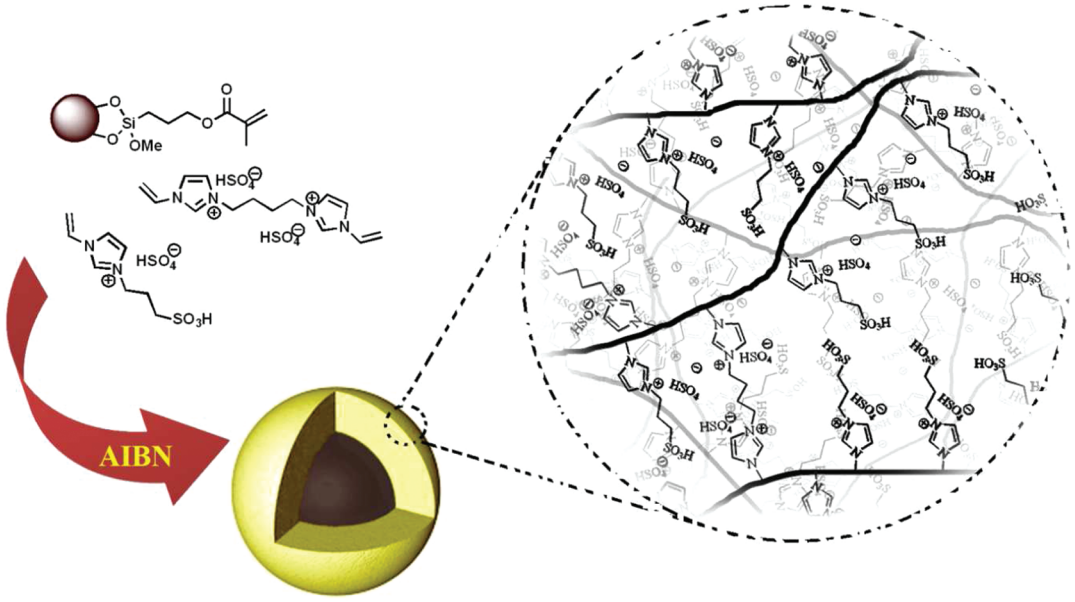


**Table 1. Recipes for the Preparation of $Fe_3O_4$@PIL with Different Polymer Content**

| sample[a] | [VSim][$HSO_4$] (mg) | [BVD] (mg) | AIBN (mg) | weight loss (wt %)[b] |
|---|---|---|---|---|
| $Fe_3O_4$@PIL(I) | 250 | 100 | 1.5 | 17 |
| $Fe_3O_4$@PIL(II) | 400 | 100 | 2.0 | 22 |
| $Fe_3O_4$@PIL(III) | 500 | 200 | 2.5 | 46 |

[a]Condition: $Fe_3O_4$ 200 mg, methanol 50 mL. [b]The weight losses were calculated from TGA curves.

methanol. The catalyst was fully characterized, and the data is presented in the Supporting Information.

**Catalyst Characterization.** In the FT-IR spectrum, bare $Fe_3O_4$ (Figure 1a) and $Fe_3O_4$@MPS (Figure 1b) show the

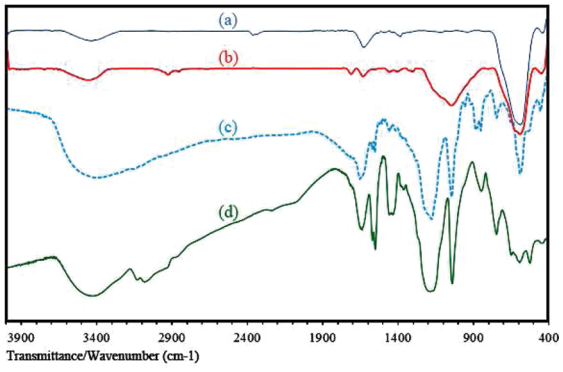


**Figure 1.** FT-IR Spectrum of (a) bare $Fe_3O_4$, (b) $Fe_3O_4$@MPS, (c) [VSim][$HSO_4$], and (d) $Fe_3O_4$@PIL.

stretching vibrations of Fe−O at 591 $cm^{-1}$. Besides, $Fe_3O_4$@MPS shows stronger stretching vibration of C═O (1712 $cm^{-1}$), C═C (1460 $cm^{-1}$), C−H (2923 $cm^{-1}$), and Si−O−Si (1035 $cm^{-1}$) than bare $Fe_3O_4$, associated to MPS functional groups. This result indicates that the MPS was successfully coated onto the surface of $Fe_3O_4$ magnetic nanoparticles.

Figure 1c shows the FT-IR spectrum of [VSim][$HSO_4$]. The characteristic peaks of [VSim][$HSO_4$] around 1035 $cm^{-1}$, 1180 $cm^{-1}$, 1557 $cm^{-1}$, 1573 $cm^{-1}$, and 1643 $cm^{-1}$ could be clearly observed and which were attributed to S═O asymmetric and symmetric stretching vibrations of the $-SO_3H$ group and C═C, C═N stretching vibrations of the imidazole ring, respectively.

In the spectrum of the $Fe_3O_4$@PIL (Figure 1d) similar peaks in (Figure 1a, b, c) could be observed. The peak at 591 $cm^{-1}$ is associated to the stretching vibrations of Fe−O in $Fe_3O_4$. Absorbance bands at 1035 $cm^{-1}$ and 1180 $cm^{-1}$ were attributed to the asymmetrical and symmetrical stretching vibrations of S═O, associated to poly([VSim][$HSO_4$]). The band at 1711 $cm^{-1}$ is related to the C═O stretching vibration for carboxylate of MPS. Therefore, it indicated that the magnetic nanoparticles were successfully coated with poly IL.

The X-ray diffraction (XRD) pattern of the $Fe_3O_4$@PIL shows characteristic peaks and relative intensities, which match well with the standard $Fe_3O_4$ sample (JCPDS file No. 19-0629, Figure 2). The broad peak from 20° to 30° is consistent with an amorphous silica phase in the shell of the $Fe_3O_4$@MPS in the catalyst.

The thermal stability of samples was investigated by thermogravimetric analysis (TGA). TGA curves for bare $Fe_3O_4$, $Fe_3O_4$@MPS, and $Fe_3O_4$@MPS@PIL are shown in Figure 3. As shown in Figure 3 in all samples, weight loss within

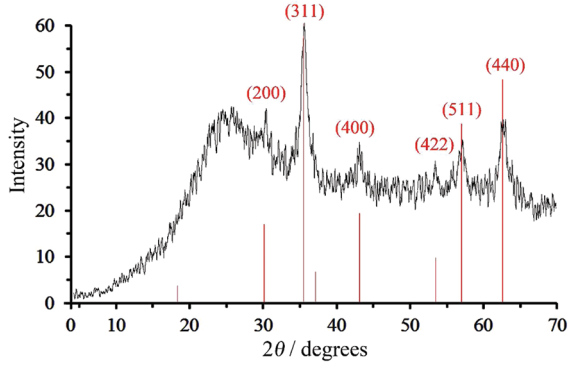


**Figure 2.** XRD pattern of $Fe_3O_4$@PIL(III).


dx.doi.org/10.1021/cs300140j | ACS Catal. 2012, 2, 1259−1266

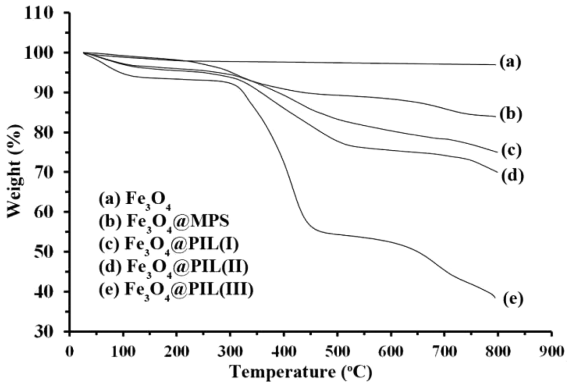


**Figure 3.** TGA of (a) bare $Fe_3O_4$, (b) $Fe_3O_4$@MPS, (c), (d), and (e) $Fe_3O_4$@PIL samples I, II, III, respectively.

200 °C was attributed completely to the loss of adsorbed water molecules. $Fe_3O_4$ coated MPS showed a higher weight loss than bare $Fe_3O_4$ because of the loss of the propylmethacrylate component in Figure 3b. From this weight loss it is calculated that the loading of the organic group bound to the silica surface was 1.02 mmol $g^{-1}$. After polymerization of multilayers of IL polymers, the weight loss in Figure 3c,d,e increased again which was due to the further increased organic components on the $Fe_3O_4$@PIL. As shown in Figure 3, the catalysts exhibited good thermal stability under 450 °C. The weight losses of $Fe_3O_4$@PILs are about 17, 22, and 46 wt % for samples I, II, III, respectively. The weight markedly decreased above 700 °C, and organic components on the $Fe_3O_4$ were decomposed completely up to 800 °C. Weight loss around 300−650 °C is attributed to -imidazolium-$(CH_2)_3SO_3H$ groups. The weight loss around 650 °C corresponded to PIL chains that are directly grafted to the surface of magnetic nanoparticles. CHN analysis of $Fe_3O_4$@PIL(III) shows 22.5% C, 5.1% H, and 7.3% N. Also, titration of $Fe_3O_4$@PIL(III) by NaOH shows the loading of proton ion in the catalyst was 2.92 mmol/g.

The SEM and TEM images of $Fe_3O_4$@PIL (III) are presented in Figure 4a,b respectively.

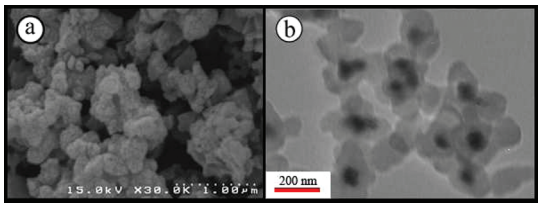


**Figure 4.** (a) SEM and (b) TEM image of $Fe_3O_4$@PIL(III).

The magnetic properties of $Fe_3O_4$@MPS and $Fe_3O_4$@PIL (III) were determined by a vibrating sample magnetometer (VSM), and magnetic hysteresis curves are shown in Figure 5. After coating with a multilayer of PIL shells, the saturation magnetization value dramatically decreased.

**Catalytic Activity of the Catalyst.** The catalytic activity of $Fe_3O_4$@PIL was studied in the synthesis of 1,1-diacetyl using the reaction between aldehydes and acetic anhydride at room temperature (Scheme 3). The corresponding acylal products were obtained in good to excellent yields (Table 2). As shown in Table 2 (Entry 5, 7, 10) hindered aldehydes and highly deactivated aldehydes (Entry 4, 6, 13) were also diacetylated with $Fe_3O_4$@PIL in excellent yield. Acid sensitive groups such as OMe and CN are stable under reaction conditions. However, 4-dimethylaminobenzaldehyde gave no diacetyl product because of the basicity of the amine groups which neutralized the acidic catalyst. We also investigated the chemoselective protection of aldehydes in the presence of ketones. As shown in Scheme 4, a 1:1 mixture of benzaldehyde and acetophenone in the presence of catalyst gave only aldehyde diacetyl. However, unfortunately both aliphatic and aromatic aldehydes showed

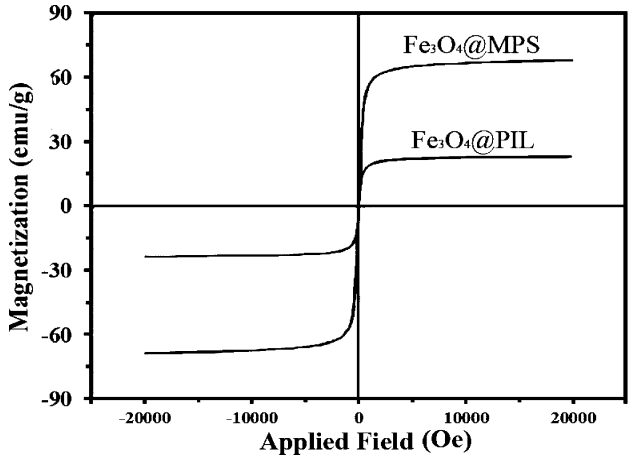


**Figure 5.** Magnetic hysteresis curves of $Fe_3O_4$@MPS and $Fe_3O_4$@PIL(III).

**Scheme 3. Acetylation of Aldehydes Using $Ac_2O$ and Their Deprotection in the Presence of $Fe_3O_4$@PIL (III) as Catalyst**

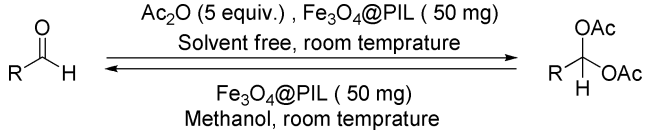


**Table 2. Acetylation of Aldehydes Using $Ac_2O$ and Their Deprotection in the Presence of $Fe_3O_4$@PIL at Room Temperature[a]**

| | | protection[b] | | deprotection[c] | |
|---|---|---|---|---|---|
| entry | R | time (min) | yield (%) | time (min) | yield (%) |
| 1 | Ph | 20 | 91 | 40 | 95 |
| 2 | 4-(Cl)Ph | 20 | 95 | 35 | 97 |
| 3 | 4-(Me)Ph | 20 | 93 | 45 | 94 |
| 4 | 4-(HO)Ph | 60 | 91 | 80 | 95 |
| 5 | 2-(HO)Ph | 60 | 97 | 80 | 98 |
| 6 | 4-(MeO)Ph | 30 | 90 | 40 | 95 |
| 7 | 2-(MeO)Ph | 120 | 87 | 60 | 94 |
| 8 | 4-($NO_2$)Ph | 10 | 98 | 15 | 100 |
| 9 | 3-($NO_2$)Ph | 10 | 94 | 15 | 99 |
| 10 | 2-($NO_2$)Ph | 60 | 95 | 10 | 100 |
| 11 | 4-($NMe_2$)Ph | 5 h | NR | - | - |
| 12 | 4-($CO_2H$)Ph | 20 | 90 | 25 | 96 |
| 13 | 4-(CN)Ph | 30 | 88 | 35 | 100 |
| 14 | vanillin | 30 | 85 | 2 h | 91 |
| 15 | furfural | 15 | 86 | 40 | 90 |
| 16 | 4-(CHO)Ph[d] | 60 | 96 | 60 | 96 |
| 17 | $^{n}$propyl | 60 | 76 | 3 h | 86 |
| 18 | $^{iso}$butyl | 60 | 82 | 3 h | 89 |

[a]Isolated yields. [b]Solvent free condition. [c]Methanol was used as solvent. GC yield. [d]Both of the aldehyde groups were converted to acylal.


dx.doi.org/10.1021/cs300140j | ACS Catal. 2012, 2, 1259−1266

**Scheme 4. Chemoslective Acetylation of Aldehydes in the Presence of Ketones**

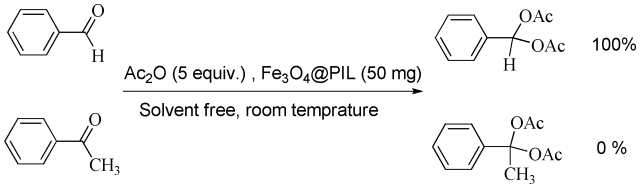


similar reactivity with $Fe_3O_4$@PIL, and no chemoselectivity was observed. We have also investigated the deprotection of acylals in methanol medium using $Fe_3O_4$@PIL as a catalyst. It was postulated that, the same catalyst in the presence of nucleophile (MeOH) would bring about deacylation via protonation of the carbonyl carbon in the acylal derivative, and the result is shown in Table 2.

Table 3 shows the data for the control experiment and optimization of solvent. Reaction between benzaldehyde and acetic anhydride was chosen for the modeling reaction, and all experiments were carried out at room temperature. As seen in Table 3 when no catalyst was used in the reaction medium, the yield of reaction was 14% in 24 h. Using bare $Fe_3O_4$ in the reaction at room temperature gave 23% yield. In another experiment using the $Fe_3O_4$@MPS gave only 12% product in 24 h. But using the $Fe_3O_4$@PIL gave 94% yield at room temperature and solvent free condition. This clearly showed that the reaction was catalyzed by multilayered poly(IL) coated magnetic nanoparticles. The effect of catalyst loading in the reaction was studied, and the result is shown in Table 3. The yield of reaction dramatically decreased when the amount of catalyst was reduced to 10 mg. The same reactions were carried out in various solvents with $Fe_3O_4$@PIL, but solvent free conditions gave the best yield. Using other catalyst for comparison gave good yield in the first run, but in the second run the activity dramatically decreased.

**Catalyst Recycling.** The recyclability of the catalyst was investigated in the syntheses of benzaldehyde 1,1-diacetate. The reaction was carried out under the same conditions 10 times (Figure 6). The completion of the reaction was monitored by thin layer chromatography (TLC). After completion of the reaction, the catalyst was magnetically separated from the reaction medium (Figure 7) and run in another reaction vessel under same condition. GC analysis showed that products were obtained in high yield even after 10 cycles. Supporting

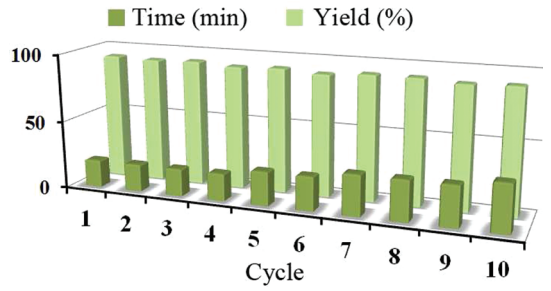


**Figure 6.** Catalyst reusability.

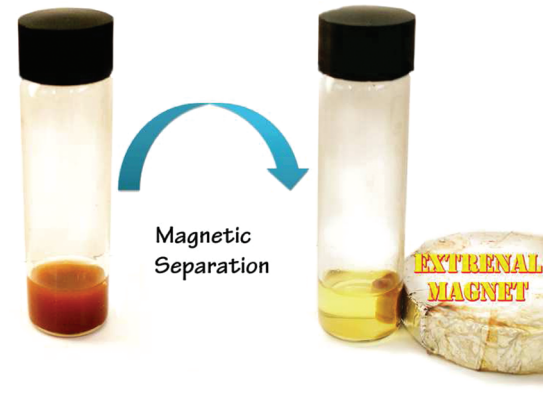


**Figure 7.** Magnetic separation of catalyst by external magnet.

**Table 3. Control Experiments of Attempted Diacetylation Reaction**[a]

| entry | catalyst | amount of catalyst (mg) | solvent | time (min) | yield[b] (%) | TOF[c,f] ($h^{-1}$) |
|---|---|---|---|---|---|---|
| 1 | | | Neat | 24 h | 14 | |
| 2 | $SiO_2/HClO_4$[d] | 100 | Neat | 15 | 98[13] | 131[17] |
| 3 | Amberlyst-15 | 500 | Neat | 2 h | 75 | 0.75 |
| | $H_2SO_4$ | 10 | Neat | 10 | 91 | 110 |
| 4 | $NH_2SO_3H$ | 50 | Neat | 60 | 94 | 4 |
| 5 | [VSim][HSO4] | 50 | Neat | 10 | 97 | 72 |
| 6 | [BVD] | 100 | Neat | 60 | 35 | 3 |
| 7 | $Fe_3O_4$ | 200 | Neat | 24 h | 23 | |
| 8 | $Fe_3O_4$@MPS | 200 | Neat | 24 h | 12 | 0.05 |
| 9 | $Fe_3O_4$@PIL[e] | 100 | Neat | 15 | 99 | 27 |
| 10 | $Fe_3O_4$@PIL | 50 | Neat | 20 | 96[92] | 40[31] |
| 11 | $Fe_3O_4$@PIL | 10 | Neat | 60 | 82 | 56 |
| 12 | $Fe_3O_4$@PIL | 50 | $CH_2Cl_2$ | 30 | 90 | 25 |
| 13 | $Fe_3O_4$@PIL | 50 | $CH_3CN$ | 30 | 86 | 24 |
| 14 | $Fe_3O_4$@PIL | 50 | $Et_2O$ | 30 | 88 | 24 |
| 15 | $Fe_3O_4$@PIL | 50 | THF | 30 | 71 | 20 |
| 16 | $Fe_3O_4$@PIL | 50 | hexane | 30 | 75 | 21 |

[a]Reaction condition; benzaldehyde (2 mmol), acetic anhydride (10 mmol), at room temperature. GC yield. [b]Fifth run. [c]TOF after fifth run. [d]Catalysts were synthesized according to reference procedures.[41] [e]Second run. [f]mmol of acidic proton in $Fe_3O_4$@PIL was calculated by titration with NaOH (2.92 mmol/g).


dx.doi.org/10.1021/cs300140j | ACS Catal. 2012, 2, 1259−1266

Information, Figure S4 in shows the FT-IR spectra of $Fe_3O_4$@PIL before and after the catalyst was used 10 times in the reaction medium. As seen in Supporting Information, Figure S4, no change in FT-IR spectra of the catalyst was observed after 10 cycles. Moreover, according to elemental analysis, the organic content in the catalyst after 10 cycles was found to be C 20.3%, H 4.4%, and N 6.1%, and no considerable changes was not seen in CHN data after recycling. Also titration of catalyst by NaOH after 10 cycles shows that the loading of proton ion was 2.75 mmol/g. To explore the catalyst leaching, the reaction of benzaldehyde (2 mmol) and $Ac_2O$ (5 mmol) catalyzed by $Fe_3O_4$@PIL (50 mg) was carried out at room temperature under solvent-free conditions. After 10 min hot ethyl acetate (5 mL) was added, and the catalyst was magnetically separated. The solution was divided into the two parts. The corresponding product of the first part was obtained with a 42% yield. The second part was reacted under the same conditions for another 10 min to afford product with 48% yield which was similar to first part and less than normal (91%; Table 2, entry 1). Therefore, these above results convinced us that the leaching of catalyst was negligible in the catalytic process. The results showed that the catalyst was recyclable, stable, and no considerable loss of catalyst efficiency had occurred after 10 cycles. It is economically suitable to the industrial application from a practical point of view. The reasons that our catalyst has a high activity and high recyclability might be that the poly(IL) chains protect nanoparticles from aggregation and provide a polar surface that reagent can react together onto the surface of the catalyst. To the best of our knowledge, this is the first acid catalyst that functionalized poly(IL) encapsulated magnetic nanoparticles which has been used in the synthesis of acylals efficiently under solvent free and room temperature conditions.

## CONCLUSION

We have developed an green catalyst and protocol for the protection of aldehydes by conversion to 1,1-diacetate in solvent free and room temperature conditions. The catalyst was synthesized by a distillation-precipitation polymerization method in the presence of magnetic nanoparticles. This synthetic method has the advantages of simple and effective polymer coating of magnetic nanoparticles. Easy magnetic separation of the catalyst eliminates the catalyst filtration process after completion of the reaction, which is an additional suitable aspect of our catalyst. Our catalyst combines the advantages of ILs and a magnetic heterogeneous catalyst. In view of the simplicity in the product separation and in the catalyst recovery and the mild reaction conditions, the present protocol could find industrial applications.

## EXPERIMENTAL SECTION

**Reagents and Analysis.** Ferric chloride hexahydrate ($FeCl_3{\cdot}6H_2O$), ammonia (30%), ferrous chloride tetrahydrate ($FeCl_2{\cdot}4H_2O$), 3-methacryloxypropyltrimethoxy-silane (MPS, 98%), and 1,3-butanesultone were obtained from Merck. 1-Vinylimidazole was obtained from Fluka and was distilled before use. 1,4-Dibromobutane was obtained from Aldrich. 2,2′ Azobisisobutyronitrile (AIBN, Kanto, 97%) was recrystallized from ethanol.

TLC was performed with silica gel 60 F254 plates, and UV light was used for visualization. FT-IR spectra of samples were taken using an ABB Bomem MB-100 FT-IR spectrophotometer. The samples were powdered and mixed with KBr to make pellets. Proton nuclear magnetic resonance spectra ($^1$H NMR) were recorded on a Bruker NMR 500 MHz instrument. TGA was acquired under a nitrogen atmosphere with a TGA Q 50 thermogravimetric analyzer. Morphology of catalyst was observed with a scanning electron microscope (SEM) instrument (Philips, XL30) Transmission electron microscopy (TEM) images were taken with a Philips EM 208 electron microscope. The magnetic property of the catalyst was measured with a vibrating sample magnetometer (VSM) (Model 7400).

**Synthesis of Magnetic Nanoparticles.** The $Fe_3O_4$ nanoparticle was synthesized by a chemical coprecipitation method of ferric and ferrous ions in alkali solution.[42] A 23.3 g portion of $FeCl_3{\cdot}6H_2O$ and 8.60 g of $FeCl_2{\cdot}4H_2O$ were dissolved in 500 mL of deionized water under nitrogen at room temperature; then 100 mL of 25% $NH_3{\cdot}H_2O$ was added with vigorous stirring. After the color of the solution turned to black, the magnetite precipitates were separated and washed several times with deionized water by magnetic decantation.

**Surface Modification of Magnetic Nanoparticles.** A 2 g portion of $Fe_3O_4$ was added to dry ethanol, followed by the addition of ammonium hydroxide 25% solution (2 mL). Afterward, excess (10 mmol per 1 g of $Fe_3O_4$) of the 3-(trimethoxysilyl)propylmethacrylate (MPS) solution was added dropwise over a period of 10 min, and the reaction mixture was stirred at 50 °C for 48 h. The particles were washed several times with methanol and magnetically separated to remove any excess of reagent and salts.

**Synthesis of Monomer ([VSim][HSO$_4$]) and Cross-Linker ([BVD]).** The synthesis route to 1-vinyl-3-(3-sulfopropyl)imidazolium hydrogen sulfate [VSim][$HSO_4$] was shown in Scheme 1; first, 3.50 g of 1,3-propanesultone (2.87 mmol) was slowly added to 2.50 g of 1-vinylimidazole (2.65 mmol) in a 50 mL round-bottom flask at 0 °C. The mixture was stirred for 24 h. Then the formed solid was washed with ether 3 times and dried in vacuum.[44] The formed solid (95% yield) was dissolved in 2 mL of $H_2O$ in a 50 mL round-bottom flask, and equimolar sulfuric acid was slowly added dropwise into the flask at 0 °C. After the dropwise addition was finished, the mixture was heated up to 60 °C gradually and then stirred for 12 h. Finally, the formed wine-colored liquid was washed with ether 3 times and dried in vacuum at 50 °C for 5 h.

1,4-Butanediyl-3,3′-bis-l-vinylimidazolium dihydrogensulfate [BVD] was synthesized according to the literature,[45] and the synthesis steps are shown in Scheme 1. For synthesis of 1,4-butanediyl-3,3′-bis-l-vinylimidazolium dihydrogensulfate [BVD] as cross-linking agent, 2.82 g (0.03 mol) of 1-vinylimidazole, 3.24 g (0.015 mol) of 1,4- dibromobutane, and 5 mL of methanol were loaded into a 50 mL round-bottom flask. The mixture was stirred at 60 °C for 15 h. After cooling down, the reaction mixture was added dropwise into 250 mL of diethyl ether. The white precipitate was filtered off and dried at room temperature until constant in weight. The product was filtered and dried in a vacuum (86% yields). For exchange of bromide anion to hydrogen sulfate, 1,4- butanediyl-3,3′-bis-l-vinyl-imidazolium dibromide was stirred by 2 equimolar of sulfuric acid in water at room temperature. Finally, the formed viscous liquid was dried in vacuum at 70 °C for 12 h.

**Synthesis of Poly(IL) Coated Magnetic Nanoparticle ($Fe_3O_4$@PIL).** The magnetic $Fe_3O_4$@PIL was prepared by distillation-precipitation polymerization of [VSim][$HSO_4$] and [BVD] as the cross-linker and AIBN as the initiator, in methanol (Scheme 2). Typically, 200 mg of $Fe_3O_4$@MPS


dx.doi.org/10.1021/cs300140j | ACS Catal. 2012, 2, 1259−1266

nanoparticles were dispersed by ultrasound in 50 mL of methanol in a 100 mL single-necked flask for 10 min. Then, a mixture of 500 mg of [VSim][$HSO_4$], 200 mg of [BVD], and 2.5 mg of AIBN were added to the flask to initiate the polymerization. The mixture was completely deoxygenated by bubbling purified nitrogen for 30 min. The flask submerged in a heating oil bath was attached with a fractionating column, Liebig condenser, and a receiver. The reaction mixture was heated from ambient temperature to the boiling state within 1 h, and the reaction was ended after about 30 mL of methanol was slowly distilled from the reaction mixture within 15 h. The obtained $Fe_3O_4$@PIL were collected by magnetic separation and washed two times with water and three times with methanol to eliminate excess reactants and few generated polymer microspheres. The resulted $Fe_3O_4$@PIL was stirred in sulfuric acid 1M to remove any uncoated $Fe_3O_4$@MPS and washed several times with water and methanol and dried in vacuum for 2 h.

**Diacetylation of Aldehydes and Deprotection of acylal.** To a magnetically stirred solution of aldehyde (2 mmol) and freshly distilled acetic anhydride (10 mmol) was added $Fe_3O_4$@PIL (50 mg) at room temperature, and the mixture was stirred until complete disappearance of the starting material (as monitored by TLC). After completion of reaction, $CH_2Cl_2$ was added and the catalyst was magnetically separated. The organic layer was washed with saturated $NaHCO_3$ (3 × 25 mL) and water (15 mL), and dried over anhydrous $Na_2SO_4$. Evaporation of the solvent under reduced pressure gave the almost pure 1,1-diacetate. Products were recrystallized in ethanol (Table 2).

For deprotection reaction, a mixture of 1,1-diacetate (2 mmol) and $Fe_3O_4$@PIL (50 mg) in methanol (5 mL) was stirred vigorously at room temperature for a specified time as required to complete the reaction (Table 2). After completion of reaction as indicated by TLC, $CH_2Cl_2$ was added, and the catalyst was magnetically separated. The organic layer was washed with water (15 mL), and dried over anhydrous $Na_2SO_4$. Evaporation of the solvent under reduced pressure gave the almost pure aldehyde.

## ■ ASSOCIATED CONTENT

### Supporting Information

Additional thermal gravimetric analysis for catalyst, IR, $^1$HNMR for monomer, cross-linker and selected products. This material is available free of charge via the Internet at http://pubs.acs.org.

## ■ AUTHOR INFORMATION

### Corresponding Author

*Phone: (982)166165311. Fax: (982)166165311. E-mail: purjavad@sharif.edu.

### Notes

The authors declare no competing financial interest.

## ■ REFERENCES

(1) Climent, M. J.; Corma, A.; Iborra, S. *Chem. Rev.* **2011**, *111*, 1072−1133.
(2) Yin, L.; Liebscher, J. *Chem. Rev.* **2007**, *107*, 133−173.
(3) Bergbreiter, D. E.; Tian, J.; Hongfa, C. *Chem. Rev.* **2009**, *109*, 530−582.
(4) Lu, J.; Toy, P. H. *Chem. Rev.* **2009**, *109*, 815−838.
(5) Gill, C. S.; Venkatasubbaiah, K.; Jones, C. W. *Adv. Synth. Catal.* **2009**, *351*, 1344−1354.
(6) Song, K.; Sauter, D. J.; Wu, J.; Dravid, V. P.; Stair, P. C. *ACS Catal.* **2012**, *2*, 384−390.
(7) Liu, G.; Liu, M.; Sun, Y.; Wang, J.; Sun, C.; Li, H. *Tetrahedron: Asymmetry* **2009**, *20*, 240−246.
(8) Joucla, L.; Cusati, G.; Pinel, C.; Djakovitch, L. *Adv. Synth. Catal.* **2010**, *352*, 1993−2001.
(9) Xu, J.; White, T.; Li, P.; He, C.; Yu, J.; Yuan, W.; Han, Y.-F. *J. Am. Chem. Soc.* **2010**, *132*, 10398−10406.
(10) Das, S.; Asefa, T. *ACS Catal.* **2011**, *1*, 502−510.
(11) Li, J.; Shi, X. Y.; Bi, Y. Y.; Wei, J. F.; Chen, Z. G. *ACS Catal.* **2011**, *1*, 657−664.
(12) Lim, C. W.; Lee, I. S. *Nano Today* **2010**, *5*, 412−434.
(13) Shekhar, M.; Wang, J.; Lee, W.; Williams, W. D.; Kim, S. M.; Stach, E. A.; Miller, J. T.; Delgass, W. N.; Ribeiro, F. H. *J. Am. Chem. Soc.* **2012**, *134*, 4700−4708.
(14) Sayah, R.; Glegola, K.; Framery, E.; Dufaud, V. *Adv. Synth. Catal.* **2007**, *349*, 373−381.
(15) Qiu, H.; Sarkar, S. M.; Lee, D. H.; Jin, M.-J. *Green Chem.* **2008**, *10*, 37−40.
(16) Yoon, H.; Ko, S.; Jang, J. *Chem. Commun.* **2007**, *14*, 1468−1470.
(17) Luo, X.; Zhang, L. *Biomacromolecules* **2010**, *11*, 2896−2903.
(18) Chien, L. J.; Lee, C. K. *Biotechnol. Bioeng.* **2008**, *100*, 223−230.
(19) Jiang, Y.; Guo, C.; Xia, H.; Mahmood, I.; Liu, C.; Liu, H. *J. Mol. Catal. B: Enzym.* **2009**, *58*, 103−109.
(20) Li, G. L.; Xu, L. Q.; Neoh, K. G.; Kang, E. T. *Macromolecules* **2011**, *44*, 2365−2370.
(21) Xuan, S.; Wang, Y. J.; Yu, J. C.; Leung, K. C. *Langmuir* **2009**, *25*, 11835−11843.
(22) Chatzipavlidis, A.; Bilalis, P.; Efthimiadou, E. K.; Boukos, N.; Kordas, G. C. *Langmuir* **2011**, *27*, 8478−8485.
(23) Taher, A.; Kim, J. B.; Jung, J. Y.; Ahn, W. S.; Jin, M. J. *Synlett* **2009**, 2477−2482.
(24) Hagiwara, H.; Sekifuji, M.; Hoshi, T.; Qiao, K.; Yokoyamac, C. *Synlett* **2007**, 1320−1322.
(25) Zhang, Y.; Zhao, Y.; Xia, C. *J. Mol. Catal. A: Chem.* **2009**, *306*, 107−112.
(26) Zhang, Y.; Xia, C. *Appl. Catal., A* **2009**, *366*, 141−147.
(27) Zhang, Q.; Su, H.; Luo, J.; Wei, Y. *Green Chem.* **2012**, *14*, 201−208.
(28) Kara, A.; Erdem, B. *J. Mol. Catal. A: Chem.* **2012**, *349*, 42−47.
(29) Gill, C. S.; Price, B. A.; Jones, C. W. *J. Catal.* **2007**, *251*, 145−152.
(30) Kirchner, B., Clare, B., Eds.; *Ionic Liquids*, 1st ed.; Springer: Heidelberg, Germany, 2009.
(31) Sahoo, S.; Kumar, P.; Lefebvre, F.; Halligudi, S. B. *Appl. Catal., A* **2009**, *354*, 17−25.
(32) Zhu, L. L.; Liu, Y. H.; Chen, J. *Ind. Eng. Chem. Res.* **2009**, *48*, 3261−3267.
(33) Chew, T. L.; Ahmad, A. L.; Bhatia, S. *Adv. Colloid Interface* **2010**, *153*, 43−57.
(34) Helminen, J.; Paatero, E. *React. Funct. Polym.* **2006**, *66*, 1021−1032.
(35) Zhang, Z.; Zhou, S.; Nie, J. *J. Mol. Catal. A: Chem.* **2007**, *265*, 9−14.
(36) Sugimura, R.; Qiao, K.; Tomida, D.; Yokoyama, C. *Catal. Commun.* **2007**, *8*, 770−772.
(37) Liu, F.; Kong, W.; Qi, C.; Zhu, L.; Xiao, F. S. *ACS Catal.* **2012**, *2*, 565−572.
(38) Kochhar, K. S.; Bal, B. S.; Deshpande, R. P.; Rajadhyaksha, S. N.; Pinnick, H. W. *J. Org. Chem.* **1983**, *48*, 1765−1767.
(39) Jin, T. S.; Sun, G.; Li, Y. W.; Li, T. S. *Green Chem.* **2002**, *4*, 255−258.
(40) Chakraborti, A. K.; Thilagavathi, R.; Kumar, R. *Synthesis* **2004**, 831−833.
(41) Khan, A. T.; Choudhury, L. H.; Ghosh, S. *J. Mol. Catal. A: Chem.* **2006**, *255*, 230−235.
(42) Liu, X. Q.; Ma, Z. Y.; Xing, J. M.; Liu, H. Z. *J. Magn. Magn. Mater.* **2004**, *270*, 1−6.

(43) Ma, W.; Xu, S.; Li, J.; Guo, J.; Lin, Y.; Wang, C. *J. Polym. Sci., Polym. Chem.* **2011**, *49*, 2725−2733.
(44) Qiao, K.; Hagiwara, H.; Yokoyama, C. *J. Mol. Catal. A: Chem.* **2006**, *246*, 65−69.
(45) Yuan, J.; Antonietti, M. *Macromolecules* **2011**, *44*, 744−750.